Electronic Supplementary Material (ESI) for CrystEngComm.

Supporting Information

Stabilization of polyiodide chains via anion···anion interactions: experiment and theory

Kevin Lamberts, Philipp Handels, Ulli Englert, Emmanuel Aubert and Enrique Espinosa

Table of Contents:

Diffraction Experiment and Refinement Results

Table 1: Experimental details.

Crystal data	
Chemical formula	$C_{36}H_{50}N_4O_{13}\cdot I_{16}$
M_r	2777.20
Crystal system, space group	Monoclinic, $P2_1$
Temperature (K)	100
a, *b*, *c* (Å)	11.8549 (13), 16.4789 (18), 17.3200 (19)
β (°)	101.091 (2)
V (Å^3)	3320.4 (6)
Z	2
Radiation type	Mo $K\alpha$
$\propto$ (mm^{-1})	7.51
Crystal size (mm)	0×.30×.20.10
Data collection	
Diffractometer	Bruker D8 Goniometer, APEX CCD Detector, Incoatec Microsource
Absorption correction	Multi-scan, *SADABS*
T_{min}, T_{max}	0.350, 0.746
No. of measured, independent and observed [$I > 2\sigma(I)$] reflections	45294, 16441, 14914
R_{int}	0.045
$(\sin \theta/\lambda)_{max}$ (Å^{-1})	0.666
Refinement	
$R[F^2 > 2\sigma(F^2)]$, $wR(F^2)$, S	0.049, 0.129, 1.00
No. of reflections	16441
No. of parameters	446
No. of restraints	1
H-atom treatment	H-atom parameters constrained
$\Delta\rho_{max}$, $\Delta\rho_{min}$ (e Å^{-3})	1.38, -1.41
Absolute structure	Classical Flack method preferred over Parson's because s.u. lower.
Absolute structure parameter	-0.04 (5)

Intensity data of the single crystal were collected on a Bruker D8 goniometer with SMART APEX CCD detector using Mo-Kα radiation (λ = 0.71074 Å) from an Incoatec microsource with multi layer optics. Temperature was controlled with an Oxford Cryostream 700. Data reduction was performed with SAINT+ and multi-scan absorption correction was applied with SADABS. The structure was solved by direct methods and refined on F^2 with SHELXL-13. Iodine atoms have been refined with anisotropic displacement parameters. Tentative assignment of anisotropic displacement parameters to non-H

atoms did not yield a significant improvement of the structure model but only resulted in a higher number of parameters as shown below:

model	C, N and O isotropic	C, N and O anisotropic
data	16441	16441
variables	446	626
restraints	1	313
R1 (all data)	0.0554	0.0551
wR2 (all data)	0.1289	0.1281
GOF	1.00	1.00
Flack parameter	0.04(5)	0.05(5)

In view of these results, the simples structure model with isotropic displacement for C, N and O atoms was preferred. All hydrogen atoms were constrained to idealized positions and included as riding with U_{iso}(H) = 1.2 U_{eq}(non-H) for C atoms, carboxy- and water-oxygen and U_{iso}(H) = 1.5 U_{eq}(non-H) for other O and N atoms. The hydrogen atoms of the water molecule were located in difference Fourier maps and and constrained to ride on the oxygen atom.

Hydrogen Bonds

Table 2: [i] -1+x,y,z; [ii] 1+x,y,-1+z; [iii] x,y,-1+z; [iv] -x,1/2+y,-z; [v] 1+x,y,z; [vi] -x,1/2+y,1-z; [vii] x,y,1+z; [viii] 1-x,1/2+y,1-z.

Donor—H···Acceptor	D—H	H···A	D···A	D—H···A
O(3)—H(1)···I(12)[ii]	0.84	2.72	3.553(11)	170
N(1)—H(8A)···O(12)[iii]	0.91	2.05	2.745(17)	132
N(1)—H(8B)···I(11)[iii]	0.91	2.84	3.641(17)	147
N(1)—H(8C)···I(3)[iv]	0.91	2.93	3.590(15)	130
O(1)—H(9)···O(5)[i]	0.84	1.81	2.649(15)	174
O(4)—H(10)···O(2)[v]	0.84	1.80	2.639(14)	175
N(2)—H(11A)···O(1W)	0.91	1.93	2.787(16)	156
N(2)—H(11B)···O(9)	0.91	1.93	2.793(16)	158
N(2)—H(11C)···I(8)[viii]	0.91	3.18	3.764(10)	124
O(6)—H(18)···I(6)	0.84	2.85	3.670(11)	164
O(9)—H(19)···I(15)[ii]	0.84	3.02	3.658(10)	134
N(3)—H(26A)···O(1W)[i]	0.91	2.01	2.830(15)	149
N(3)—H(26B)···O(6)	0.91	2.01	2.815(16)	147
N(3)—H(26C) ···I(5)[vi]	0.91	3.00	3.843(12)	155
O(7)—H(27)···O(11)[i]	0.84	1.79	2.630(14)	174
O(1W)—H(28A)···I(6)[v]	0.97	2.70	3.610(11)	156
O(1W)—H(28A)···O(5)	0.97	2.36	2.864(14)	112
O(1W)—H(28B)···I(16)[ii]	0.97	2.59	3.517(11)	161
O(10)—H(29)···O(8)[v]	0.84	1.86	2.696(15)	172
N(4)—H(30A) ···I(3)[viii]	0.91	2.69	3.574(13)	164
N(4)—H(30B) ···I(11)[v]	0.91	2.78	3.595(13)	150
N(4)—H(30C)···O(3)[vii]	0.91	2.00	2.811(16)	148
O(12)—H(37)···I(10)	0.82	2.87	3.617(10)	153

IR spectrum

The IR spectrum was measured on a KBr pellet with a Nicolet Avatar 360 E.S.P. spectrometer.

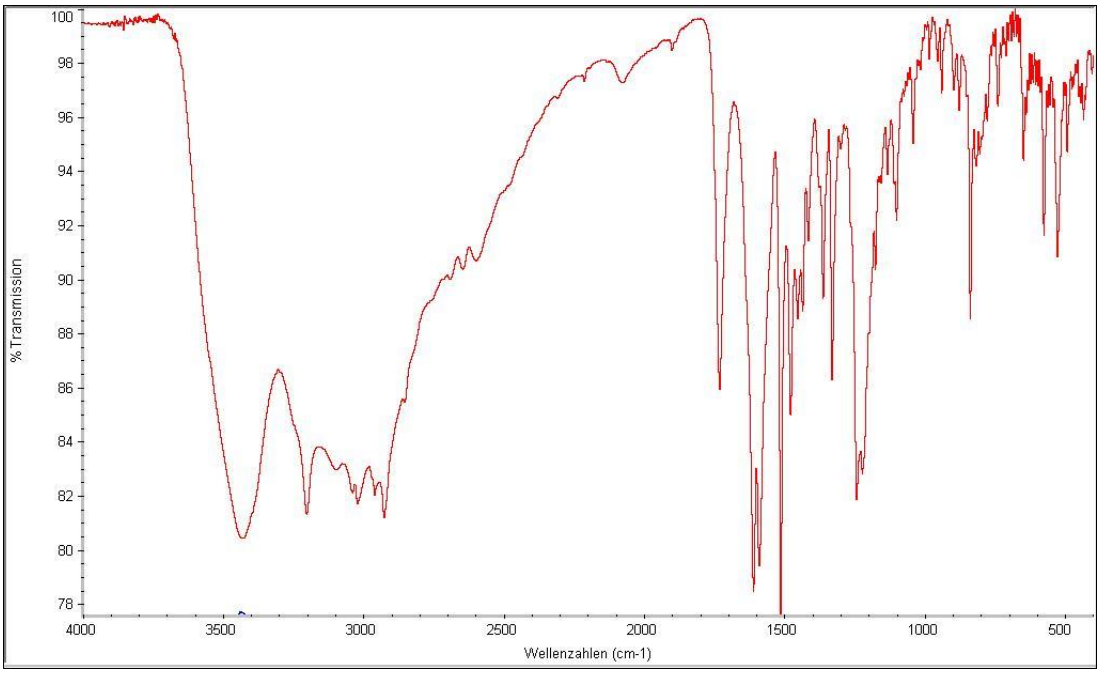

Figure 1: IR spectrum of **1**.

Raman spectrum

The Raman spectrum was obtained with a Horiba LABRAM HR instrument equipped with a 633 nm HeNe excitation laser.

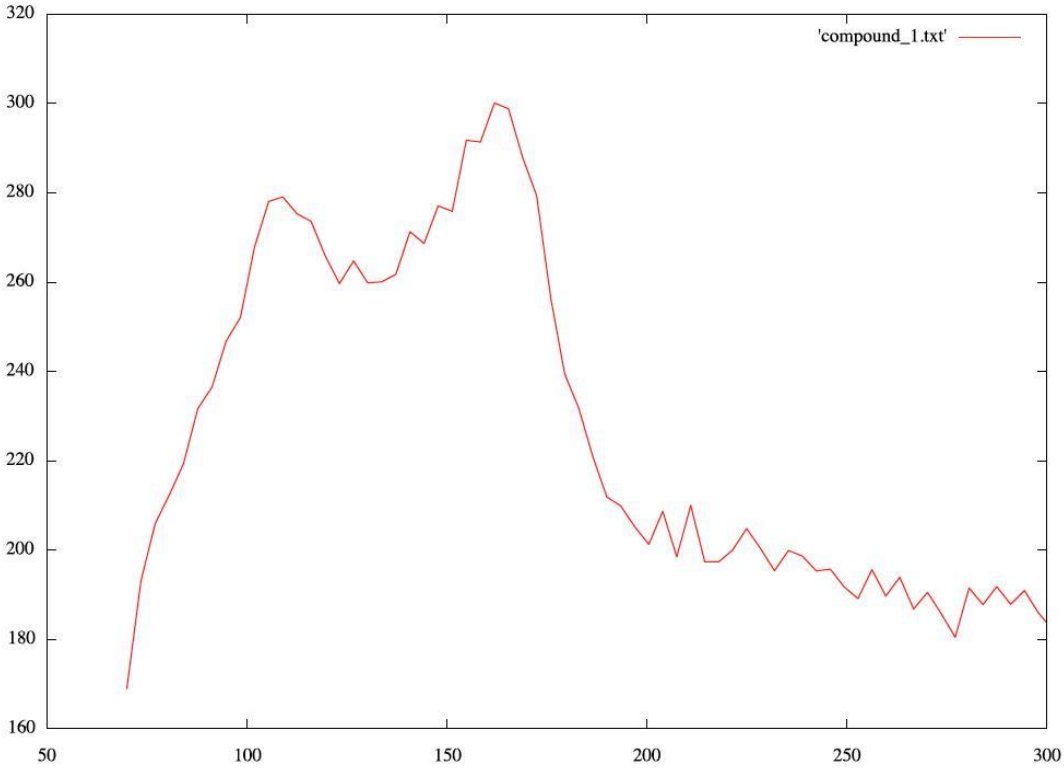

Figure 2: Raman spectrum of **1.**

Theoretical calculations

Density Functional Theory calculations were performed using the Gaussian09 software[1] at the MP2 level. The aug-cc-pVTZ basis set was used, together with a pseudopotential for iodine atoms.[2] Topological analyses were done with AIMAll software package.[3]

For all figures displaying Laplacian properties ($\nabla^2\rho$) the following conventions are used:

-isocontours of $\nabla^2\rho$ are blue dashed lines for positive values and red solid lines for negative values

-L=-$\nabla^2\rho$ critical points are displayed as colored spheres:

(3,-3) yellow

(3,-1) dark green

(3,+1) pink

(3,+3) cyan

1) I_2, I_3^- monomers

I_2, I_3^- monomers were optimized and frequency calculations were performed in order to check that true energy minima were found.

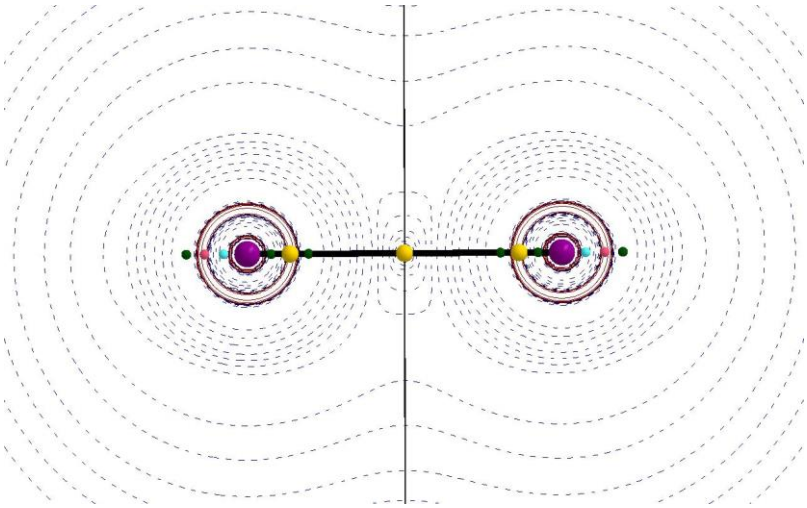

Figure 3: Laplacian map ($\nabla^2\rho$) in the plane of the I_2 monomer. Bond paths are displayed as solid black lines and interatomic surfaces as thin black lines.

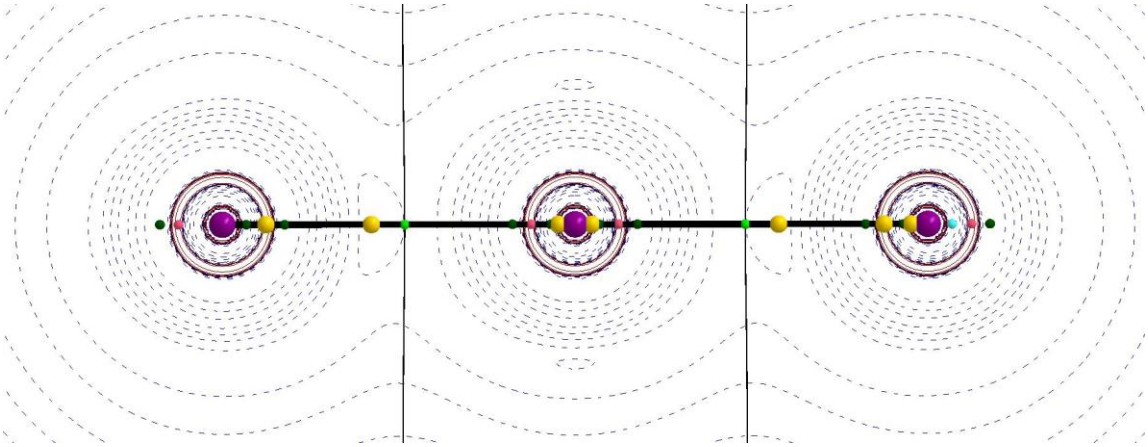

Figure 4: Laplacian map ($\nabla^2\rho$) in the plane of the I_3^- monomer. Bond paths are displayed as solid black lines and interatomic surfaces as thin black lines.

	$d(L_{CP}\cdots\rho_{CP})$(Å)	ρ (a.u.)	$\nabla^2\rho$ (a.u.)	Q (*e*)[a]
I_2	0	0.078230	-0.000550	0 / 0
I_3^-	0.276 / 0.276	0.063815 / 0.063815	+0.030539 / +0.030539	-0.492 / -0.016 / -0.492

[a] : Integrated charges of atoms as they appear on the corresponding figures, from left to right.

Table 3. Topological properties at the $L=-\nabla^2\rho$ (3,-3) interatomic critical points of I_2 and I_3^- monomers.

2) I_2, I_3^- dimers at experimental geometry

I_i		I14	I15	I16	I1	I2
Q (*e*) [a]		-0.413	-0.004	-0.432	+0.042	-0.192
$\nabla^2\rho$ (a.u.) [b]	I_{i-1}-I_i	N/A N/A	/ /	+0.032213 /	/ /	+0.014734 /
	I_i-I_{i+1}	+0.028231 /	/ /	+0.035028 +0.026134	/ /	N/A N/A
d($L_{CP}\cdots\rho_{CP}$)(Å)	I_{i-1}-I_i	N/A N/A	/ /	0.326 /	/ /	0.117 /
	I_i-I_{i+1}	0.239 /	/ /	0.649 0.146	/ /	N/A N/A
	[a] : Integrated charges of atoms [b] : Laplacian value at the L=-$\nabla^2\rho$ interatomic critical points					

Table 4. Topological and geometrical properties at the L=-$\nabla^2\rho$ interatomic critical points of the I14-I15-I16···I1-I2 dimer. First and second lines correspond to values observed at (3,-3) and (3,+1) CP's, respectively.

I_i		I1	I2	I3	I4	I5
Q (*e*) [a]		-0.257	+0.019	-0.486	+0.010	-0.286
$\nabla^2\rho$ (a.u.) [b]	I_{i-1}-I_i	N/A N/A	/ /	/ +0.035781	/ /	+0.021594 /
	I_i-I_{i+1}	+0.019114 /	/ /	/ +0.037502	/ /	N/A N/A
d($L_{CP}\cdots\rho_{CP}$)(Å)	I_{i-1}-I_i	N/A N/A	/ /	/ 0.239	/ /	0.162 /
	I_i-I_{i+1}	0.144 /	/ /	/ 0.307	/ /	N/A N/A
	[a] : Integrated charges of atoms [b] : Laplacian value at the L=-$\nabla^2\rho$ interatomic critical points					

Table 5. Topological and geometrical properties at the L=-$\nabla^2\rho$ interatomic critical points of the I1-I2··· I3-I4-I5 dimer. First and second lines correspond to values observed at (3,-3) and (3,+1) CP's, respectively.

I_i		I3	I4	I5	I6	I7	I8
Q (*e*)[a]		-0.738	-0.058	-0.245	-0.469	-0.008	-0.482
$\nabla^2\rho$ (a.u.) [b]	I_{i-1}-I_i	N/A N/A	/ /	+0.022151 /	+0.043032 +0.030317	/ /	+0.030288 /
	I_i-I_{i+1}	+0.035715 /	/ /	/ /	+0.030901 /	/ /	N/A N/A
d(L_{CP}···ρ_{CP})(Å)	I_{i-1}-I_i	N/A N/A	/ /	0.135 /	0.701 0.079	/ /	0.257 /
	I_i-I_{i+1}	0.433 /	/ /	/ /	0.294 /	/ /	N/A N/A
	[a] : Integrated charges of atoms [b] : Laplacian value at the L=-$\nabla^2\rho$ interatomic critical points						

Table 6. Topological and geometrical properties at the L=-$\nabla^2\rho$ interatomic critical points of the I3-I4-I5···I6-I7-I8 dimer. First and second lines correspond to values observed at (3,-3) and (3,+1) CP's, respectively.

I_i		I6	I7	I8	I9	I10	I11
Q (*e*)[a]		-0.537	-0.005	-0.421	-0.229	-0.056	-0.752
$\nabla^2\rho$ (a.u.) [b]	I_{i-1}-I_i	N/A N/A	/ /	+0.029578 /	/ /	/ /	+0.035778 +0.036425
	I_i-I_{i+1}	+0.031410 /	/ /	+0.043232 +0.031551	+0.021550 /	/ /	N/A N/A
d(L_{CP}···ρ_{CP})(Å)	I_{i-1}-I_i	N/A N/A	/ /	0.251 /	/ /	/ /	0.447 0.279
	I_i-I_{i+1}	0.302 /	/ /	0.718 0.079	0.126 /	/ /	N/A N/A
	[a] : Integrated charges of atoms [b] : Laplacian value at the L=-$\nabla^2\rho$ interatomic critical points						

Table 7. Topological and geometrical properties at the L=-$\nabla^2\rho$ interatomic critical points of the I6-I7-I8···I9-I10-I11 dimer. First and second lines correspond to values observed at (3,-3) and (3,+1) CP's, respectively.

I_i		I9	I10	I11	I12	I13
Q (*e*)[a]		-0.278	+0.013	-0.527	+0.023	-0.231
$\nabla^2\rho$ (a.u.) [b]	I_{i-1}-I_i	N/A N/A	/ /	/ +0.035240	/ /	+0.017368 /
	I_i-I_{i+1}	+0.020917 /	/ /	/ +0.030955	/ /	N/A N/A
$d(L_{CP}\cdots\rho_{CP})$(Å)	I_{i-1}-I_i	N/A N/A	/ /	/ 0.274	/ /	0.132 /
	I_i-I_{i+1}	0.157 /	/ /	/ 0.186	/ /	N/A N/A
	[a] : Integrated charges of atoms [b] : Laplacian value at the L=-$\nabla^2\rho$ interatomic critical points					

Table 8. Topological and geometrical properties at the L=-$\nabla^2\rho$ interatomic critical points of the I9-I10-I11⋯ I12-I13 dimer. First and second lines correspond to values observed at (3,-3) and (3,+1) CP's, respectively.

I_i		I12	I13	I14	I15	I16
Q (*e*)[a]		-0.198	+0.043	-0.387	-0.005	-0.453
$\nabla^2\rho$ (a.u.) [b]	I_{i-1}-I_i	N/A N/A	/ /	+0.034627 +0.029802	/ /	+0.029420 /
	I_i-I_{i+1}	+0.014518 /	/ /	+0.031888 /	/ /	N/A N/A
$d(L_{CP}\cdots\rho_{CP})$(Å)	I_{i-1}-I_i	N/A N/A	/ /	0.618 0.162	/ /	0.267 /
	I_i-I_{i+1}	0.119 /	/ /	0.289 /	/ /	N/A N/A
	[a] : Integrated charges of atoms [b] : Laplacian value at the L=-$\nabla^2\rho$ interatomic critical points					

Table 9. Topological and geometrical properties at the L=-$\nabla^2\rho$ interatomic critical points of the I12-I13⋯I14-I15-I16 dimer. First and second lines correspond to values observed at (3,-3) and (3,+1) CP's, respectively.

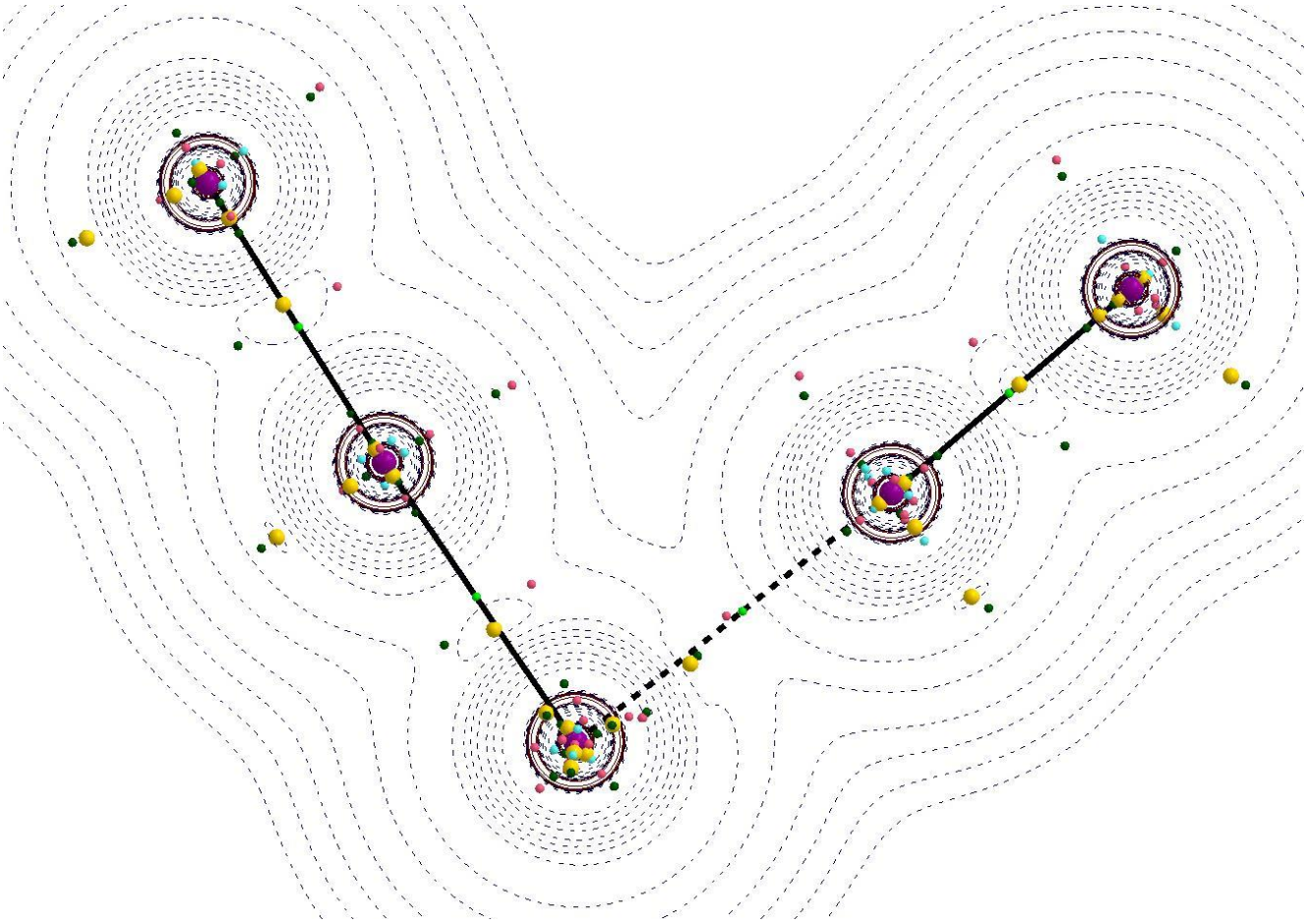

Figure 5: Laplacian map ($\nabla^2\rho$) in the plane of the I14-I15-I16···I1-I2 dimer (in the figure, atoms are placed from left to right) together with positions of ρ and $\nabla^2\rho$ critical points.

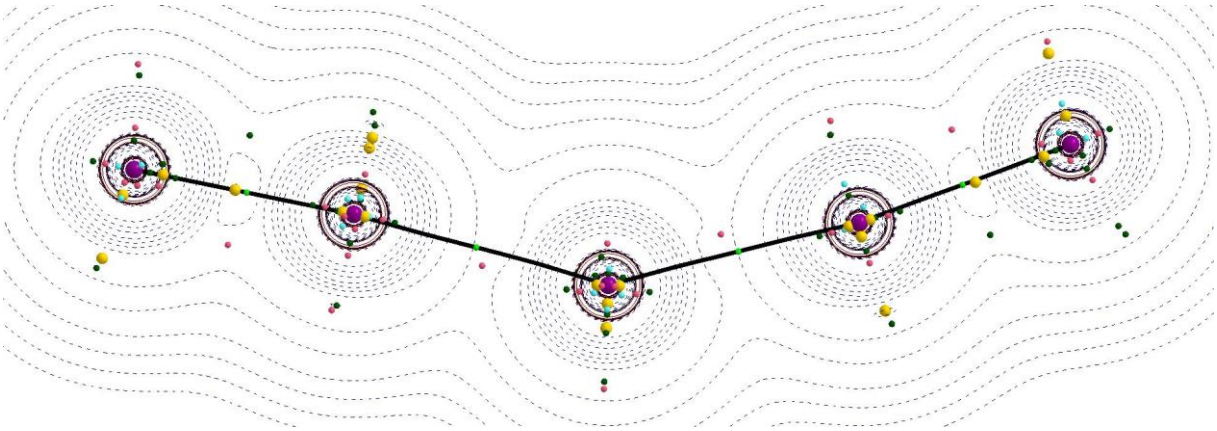

Figure 6: Laplacian map ($\nabla^2\rho$) in the plane of the I1-I2···I3-I4-I5 dimer (in the figure, atoms are placed from left to right) together with positions of ρ and $\nabla^2\rho$ critical points.

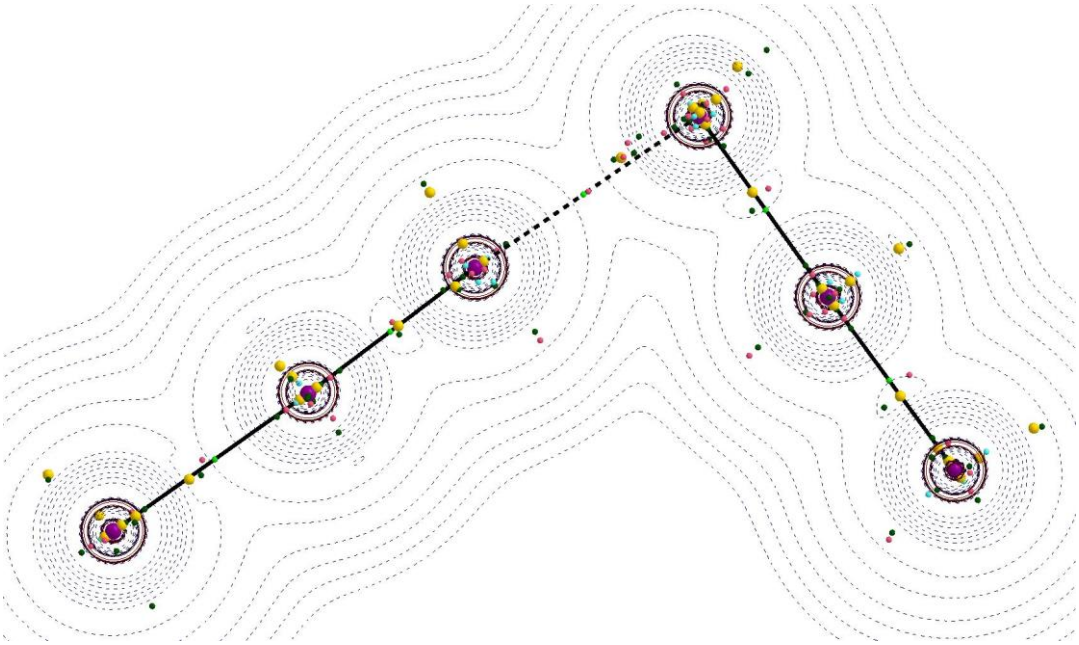

Figure 7: Laplacian map ($\nabla^2\rho$) in the plane of theI3-I4-I5···I6-I7-I8 dimer (in the figure, atoms are placed from left to right) together with positions of ρ and $\nabla^2\rho$ critical points.

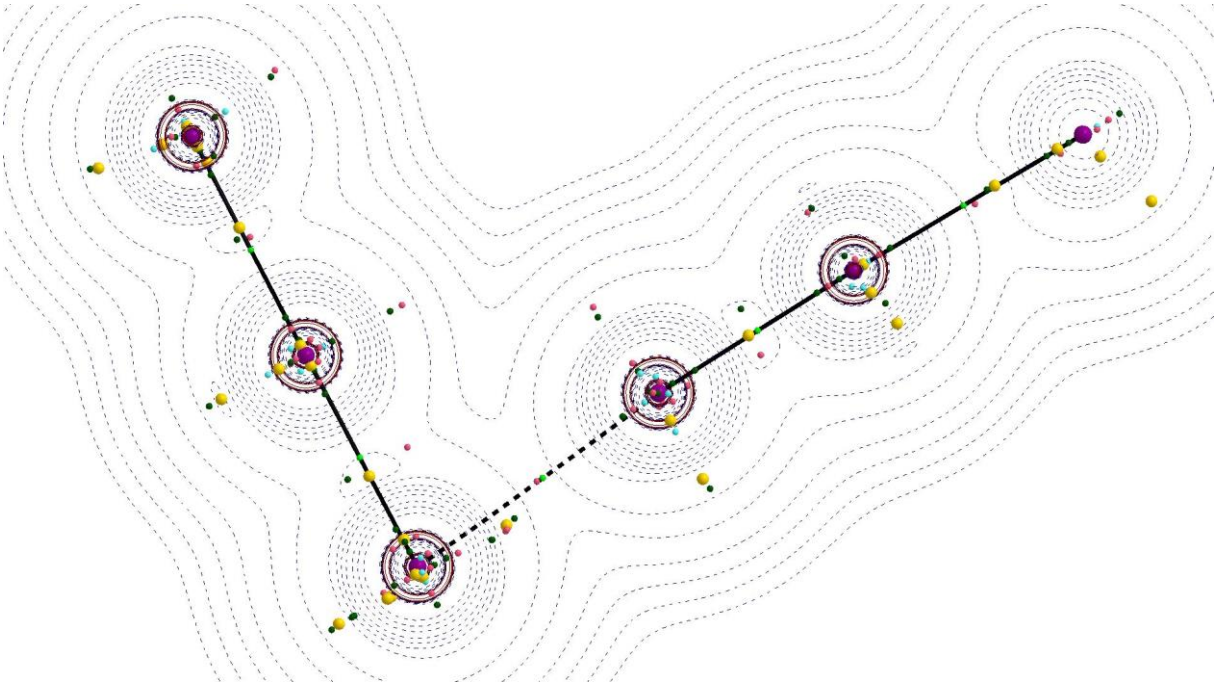

Figure 8: Laplacian map ($\nabla^2\rho$) in the plane of the I6-I7-I8···I9-I10-I11 dimer (in the figure, atoms are placed from left to right) together with positions of ρ and $\nabla^2\rho$ critical points.

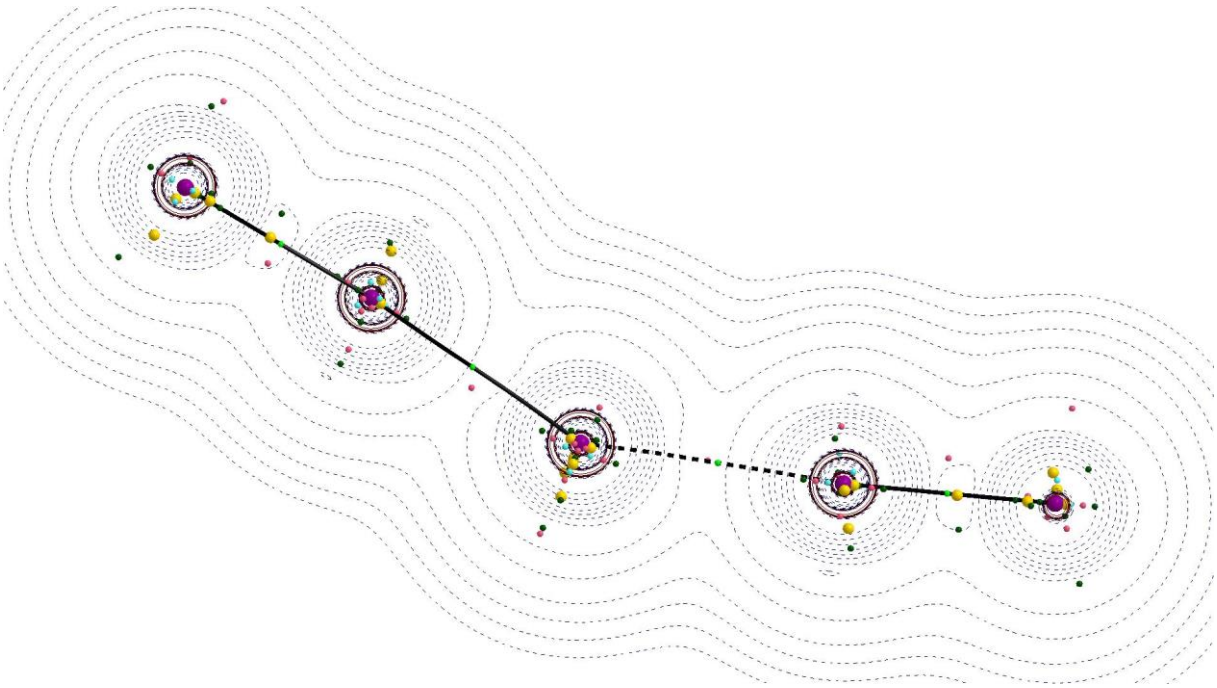

Figure 9: Laplacian map ($\nabla^2\rho$) in the plane of the I9-I10-I11···I12-I13 dimer (in the figure, atoms are placed from left to right) together with positions of ρ and $\nabla^2\rho$ critical points.

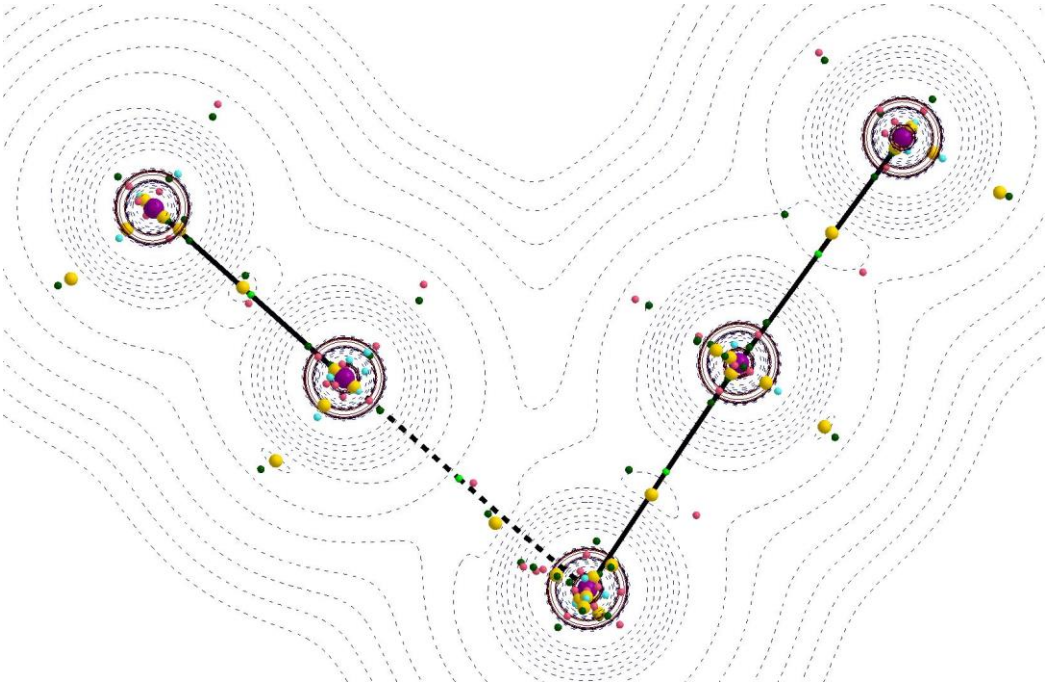

Figure 10: Laplacian map ($\nabla^2\rho$) in the plane of the I12-I13···I14-I15-I16 dimer (in the figure, atoms are placed from left to right) together with positions of ρ and $\nabla^2\rho$ critical points.

3) I_2, I_3^- trimers at experimental geometry

I_i		I9	I10	I11	I12	I13	I14	I15	I16
Q (*e*)[a]		-0.361	-0.001	-0.527	-0.095	-0.093	-0.413	-0.005	-0.499
$\nabla^2\rho$ (a.u.) [b]	I_{i-1}-I_i	N/A N/A	/ /	/ +0.031741	/ /	+0.017383 /	+0.039118 +0.034953	/ /	+0.030473 /
	I_i-I_{i+1}	+0.025344 /	/ /	/ +0.036524	/ /	/ /	+0.030782	/ /	N/A N/A
d(L_{CP}···ρ_{CP})(Å)	I_{i-1}-I_i	N/A N/A	/ /	/ 0.370	/ /	0.016 /	0.642 0.119	/ /	0.287 /
	I_i-I_{i+1}	0.187 /	/ /	/ 0.107	/ /	/ /	0.271 /	/ /	N/A N/A
	[a] : Integrated charges of atoms [b] : Laplacian value at the L=-$\nabla^2\rho$ interatomic critical points								

Table 10. Topological and geometrical properties at the L=-$\nabla^2\rho$ interatomic critical points of the I9-I10-I11···I12-I13···I14-I15-I16 trimer. First and second lines correspond to values observed at (3,-3) and (3,+1) CP's, respectively.

I_i		I1	I2	I3	I4	I5	I6	I7	I8
Q (*e*)[a]		-0.338	+0.001	-0.504	-0.080	-0.142	-0.469	-0.006	-0.462
$\nabla^2\rho$ (a.u.) [b]	I_{i-1}-I_i	N/A N/A	/ /	/ +0.032058	/ /	+0.020574 /	+0.040327 +0.028427	/ /	+0.029430 /
	I_i-I_{i+1}	+0.023543 /	/ /	/ +0.044355	/ /	/ /	+0.031344 /	/ /	N/A N/A
d(L_{CP}···ρ_{CP})(Å)	I_{i-1}-I_i	N/A N/A	/ /	/ 0.320	/ /	0.056 /	0.697 0.100	/ /	0.251 /
	I_i-I_{i+1}	0.175 /	/ /	/ 0.173	/ /	/ /	0.305 /	/ /	N/A N/A
	[a] : Integrated charges of atoms [b] : Laplacian value at the L=-$\nabla^2\rho$ interatomic critical points								

Table 11. Topological and geometrical properties at the L=-$\nabla^2\rho$ interatomic critical points of the I1-I2···I3-I4-I5···I6-I7-I8 trimer. First and second lines correspond to values observed at (3,-3) and (3,+1) CP's, respectively.

I_i		I6	I7	I8	I9	I10	I11	I12	I13
Q (*e*)[a]		-0.519	-0.005	-0.420	-0.133	-0.075	-0.542	+0.005	-0.311
$\nabla^2\rho$ (a.u.) [b]	I_{i-1}-I_i	N/A N/A	/ /	+0.030213 /	/ /	/ /	/ +0.041309	/ /	N/A N/A
	I_i-I_{i+1}	+0.030799 /	/ /	+0.040677 +0.029847	+0.019782 /	/ /	/ +0.027885	/ /	+0.021958 /
d(L_{CP}···ρ_{CP})(Å)	I_{i-1}-I_i	N/A N/A	/ /	0.258 /	/ /	/ /	/ 0.148	/ /	0.164 /
	I_i-I_{i+1}	0.295 /	/ /	0.708 0.098	0.051 /	/ /	/ 0.295	/ /	N/A N/A
	[a] : Integrated charges of atoms [b] : Laplacian value at the L=-$\nabla^2\rho$ interatomic critical points								

Table 12. Topological and geometrical properties at the L=-$\nabla^2\rho$ interatomic critical points of the I6-I7-I8···I9-I10-I11···I12-I13 trimer. First and second lines correspond to values observed at (3,-3) and (3,+1) CP's, respectively.

I_i		I14	I15	I16	I1	I2	I3	I4	I5
Q (*e*)[a]		-0.459	-0.008	-0.459	-0.115	-0.086	-0.490	-0.012	-0.371
$\nabla^2\rho$ (a.u.) [b]	I_{i-1}-I_i	N/A N/A	/ /	+0.031563 /	/ /	+0.018708 /	/ +0.042176	/ /	+0.026047 /
	I_i-I_{i+1}	+0.029616 /	/ /	+0.039580 +0.031178	/ /	/ /	+0.032546 /	/ /	N/A N/A
$d(L_{CP}\cdots\rho_{CP})$(Å)	I_{i-1}-I_i	N/A N/A	/ /	0.304 /	/ /	0.027 /	/ 0.131	/ /	0.192 /
	I_i-I_{i+1}	0.256 /	/ /	0.664 0.109	/ /	/ /	0.216	/ /	N/A N/A
	[a] : Integrated charges of atoms [b] : Laplacian value at the $L=-\nabla^2\rho$ interatomic critical points								

Table 13. Topological and geometrical properties at the $L=-\nabla^2\rho$ interatomic critical points of the I14-I15-I15···I1-I2···I3-I4-I5 trimer. First and second lines correspond to values observed at (3,-3) and (3,+1) CP's, respectively.

I_i		I3	I4	I5	I6	I7	I8	I9	I10	I11
Q (*e*)[a]		-0.762	-0.072	-0.022	-0.471	+0.003	-0.430	-0.204	-0.068	-0.775
$\nabla^2\rho$ (a.u.) [b]	I_{i-1}-I_i	N/A N/A	/ /	+0.021722 /	+0.041334 +0.029512	/ /	+0.030272 /	/ /	/ /	+0.036789 /
	I_i-I_{i+1}	+0.036808 /	/ /	/ /	+0.031233 /	/ /	+0.041743 +0.030823	+0.021055 /	/ /	N/A N/A
$d(L_{CP}\cdots\rho_{CP})$(Å)	I_{i-1}-I_i	N/A N/A	/ /	0.115 /	0.698 0.091	/ /	0.256 /	/ /	/ /	0.458 /
	I_i-I_{i+1}	0.442 /	/ /	/ /	0.299 /	/ /	0.714 0.089	0.107 /	/ /	N/A N/A
	[a] : Integrated charges of atoms [b] : Laplacian value at the L=-$\nabla^2\rho$ interatomic critical points									

Table 14. Topological and geometrical properties at the L=-$\nabla^2\rho$ interatomic critical points of the I3-I4-I5···I6-I7-I8···I9-I10-I11 trimer. First and second lines correspond to values observed at (3,-3) and (3,+1) CP's, respectively.

I_i		I12	I13	I14	I15	I16	I1	I2
Q (*e*)[a]		-0.185	+0.040	-0.343	+0.012	-0.385	+0.040	-0.179
$\nabla^2\rho$ (a.u.) [b]	I_{i-1}-I_i	N/A N/A	/ /	+0.034502 +0.030412	/ /	+0.030516 /	/ /	+0.014227 /
	I_i-I_{i+1}	+0.014092 /	/ /	+0.029890 /	/ /	+0.034864 +0.026700	/ /	N/A N/A
d($L_{CP}\cdots\rho_{CP}$)(Å)	I_{i-1}-I_i	N/A N/A	/ /	0.628 0.156	/ /	0.306 /	/ /	0.110 /
	I_i-I_{i+1}	0.112 /	/ /	0.272 /	/ /	0.661 0.142	/ /	N/A N/A
	[a] : Integrated charges of atoms [b] : Laplacian value at the L=-$\nabla^2\rho$ interatomic critical points							

Table 15. Topological and geometrical properties at the L=-$\nabla^2\rho$ interatomic critical points of the I12-I13···I14-I15-I16···I1-I2 trimer. First and second lines correspond to values observed at (3,-3) and (3,+1) CP's, respectively.

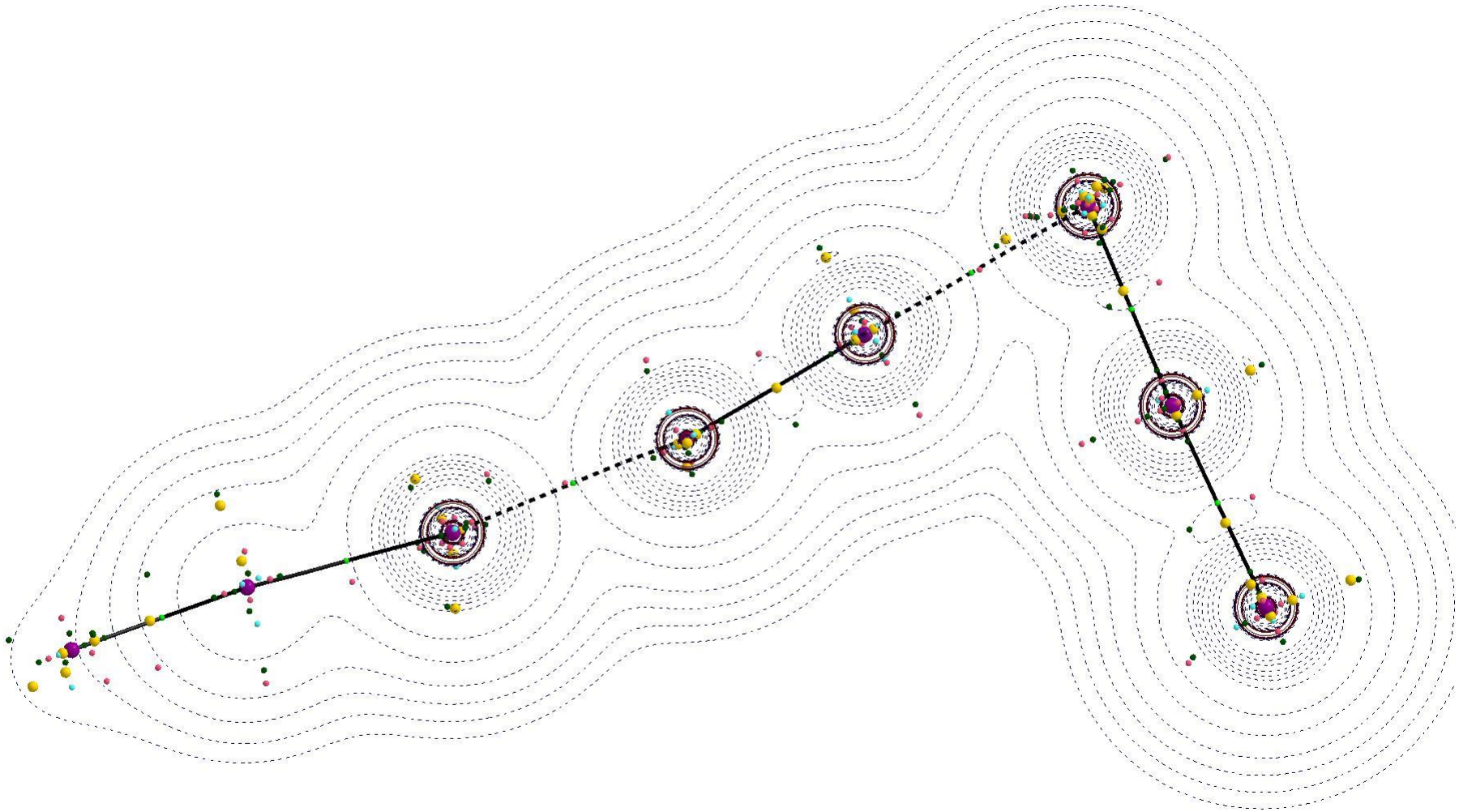

Figure 11: Laplacian map ($\nabla^2\rho$) in the plane of the I9-I10-I11···I12-I13···I14-I15-I16 trimer (in the figure, atoms are placed from left to right) together with positions of ρ and $\nabla^2\rho$ critical points.

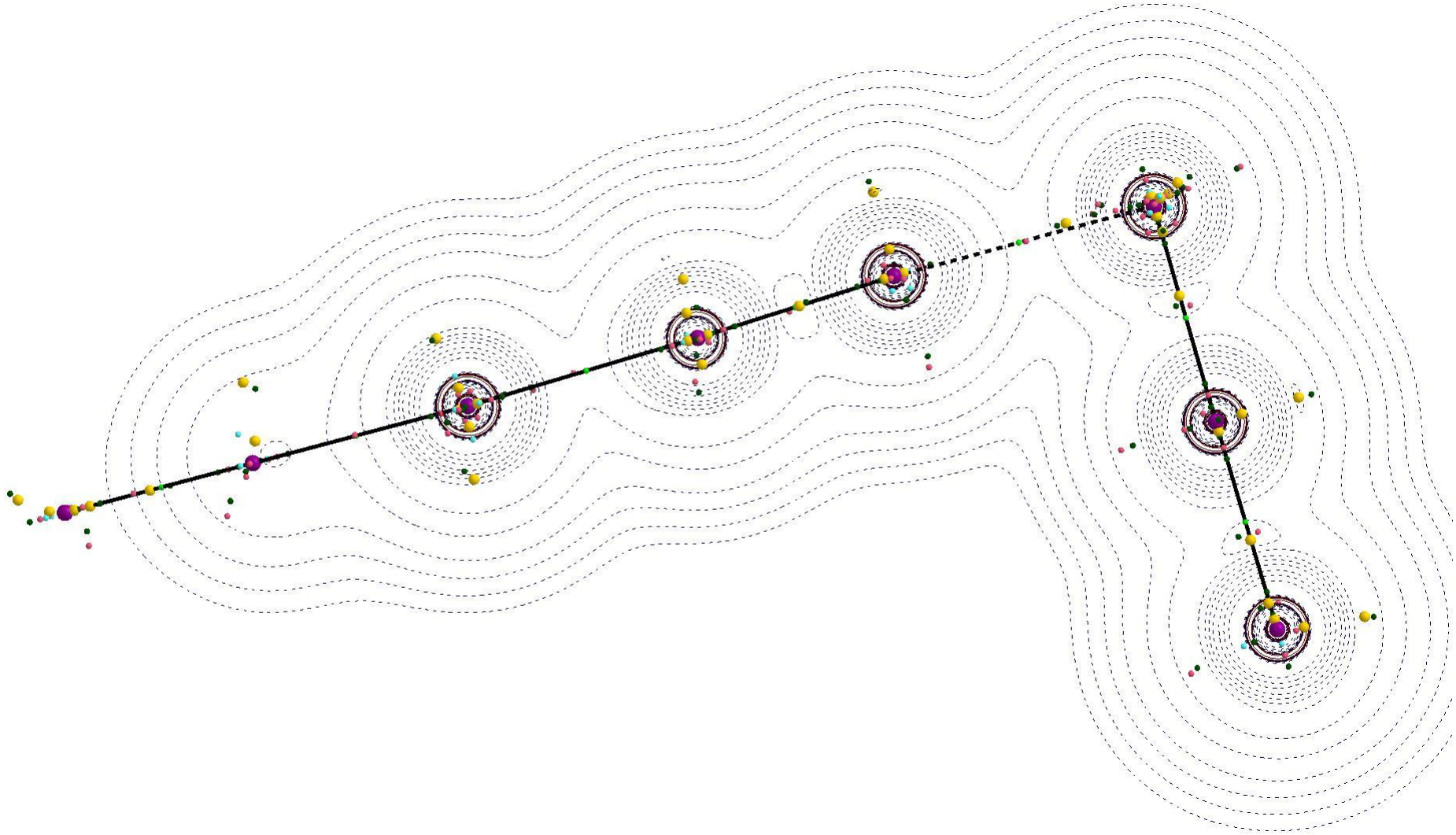

Figure 12: Laplacian map ($\nabla^2\rho$) in the plane of the I1-I2···I3-I4-I5···I6-I7-I8 trimer (in the figure, atoms are placed from left to right) together with positions of ρ and $\nabla^2\rho$ critical points.

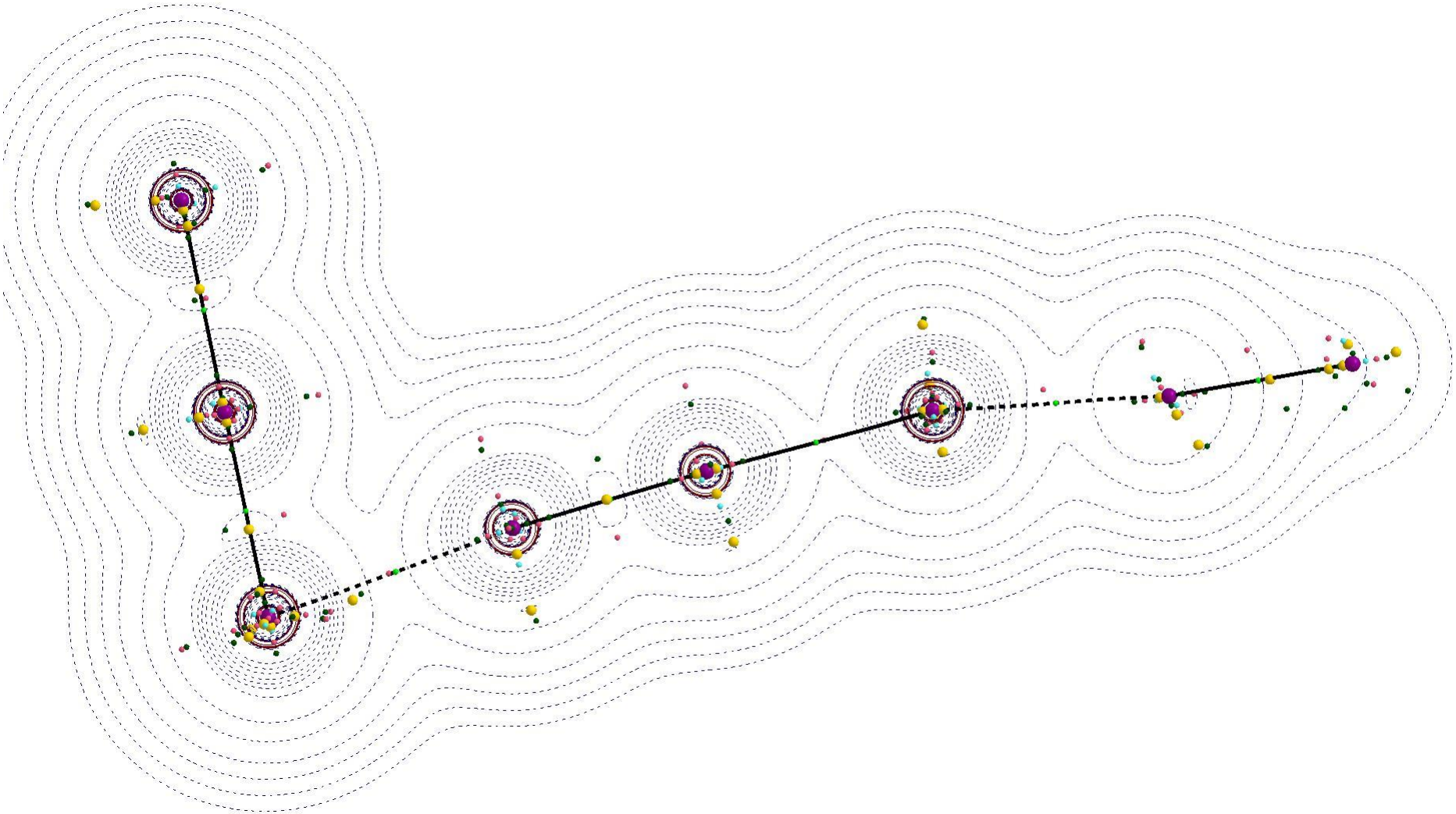

Figure 13: Laplacian map ($\nabla^2\rho$) in the plane of the I6-I7-I8···I9-I10-I11···I12-I13 trimer (in the figure, atoms are placed from left to right) together with positions of ρ and $\nabla^2\rho$ critical points.

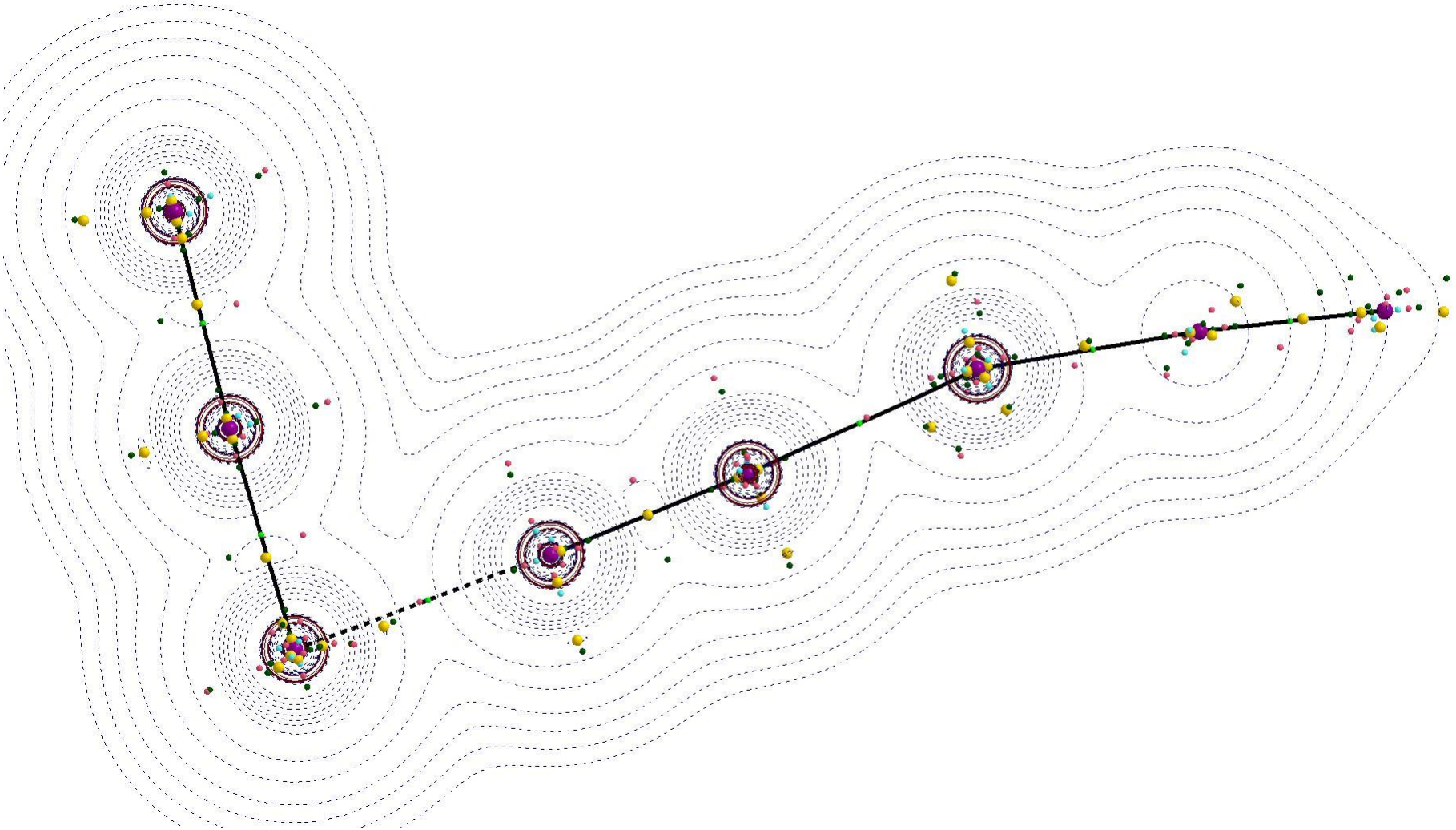

Figure 14: Laplacian map ($\nabla^2\rho$) in the plane of the I14-I15-I16···I1-I2···I3-I4-I5 trimer (in the figure, atoms are placed from left to right) together with positions of ρ and $\nabla^2\rho$ critical points.

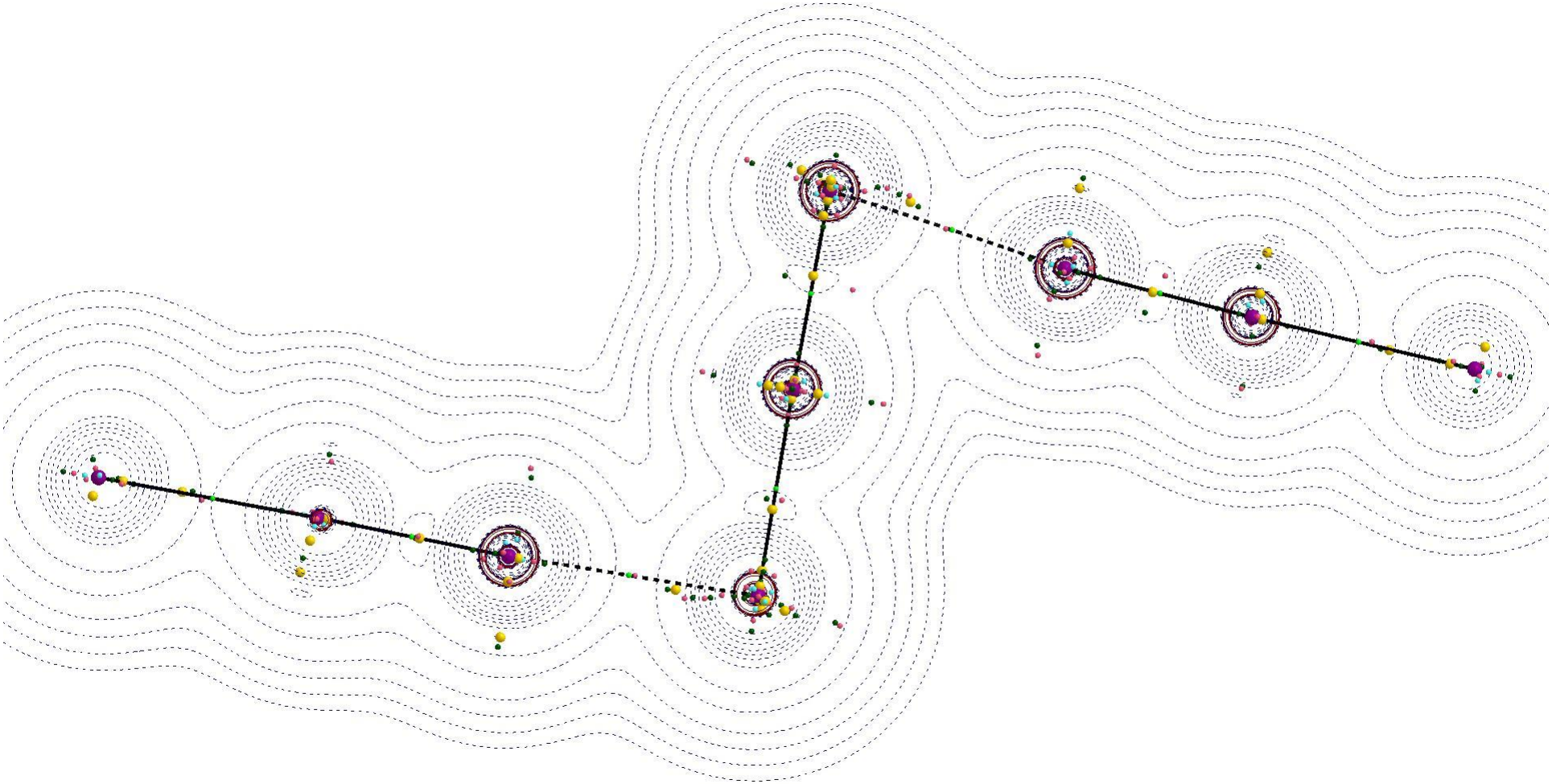

Figure 15: Laplacian map ($\nabla^2\rho$) in the plane of the I3-I4-I5···I6-I7-I8···I9-I10-I11 trimer (in the figure, atoms are placed from left to right) together with positions of ρ and $\nabla^2\rho$ critical points.

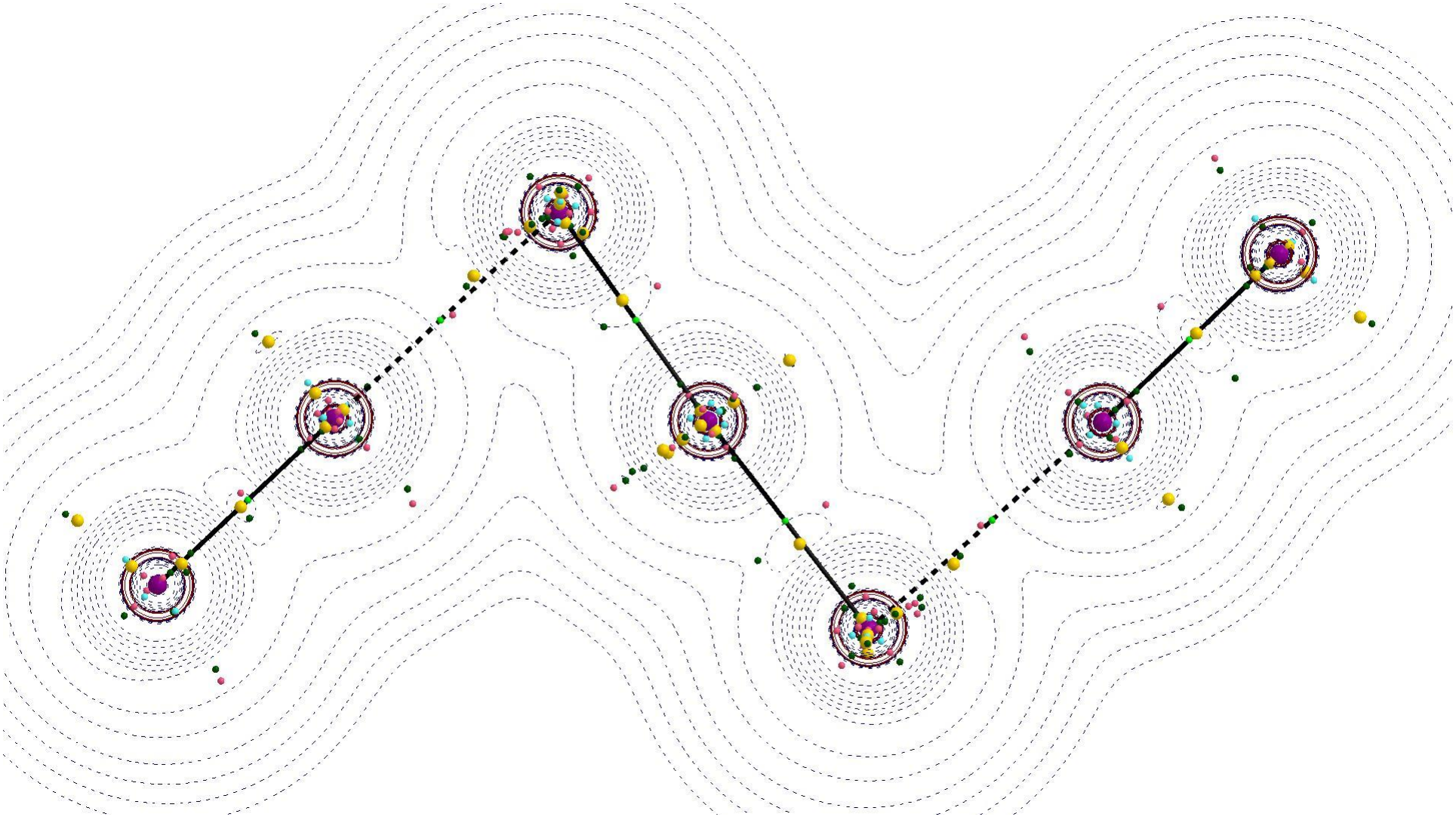

Figure 16: Laplacian map ($\nabla^2\rho$) in the plane of the I12-I13···I14-I15-I16···I1-I2 trimer (in the figure, atoms are placed from left to right) together with positions of ρ and $\nabla^2\rho$ critical points.

4) Chains at experimental geometry

I_i		I1	I2	I3	I4	I5	I6	I7	I8
Q (*e*)[a]		-0.369 -0.208	-0.010 -0.010	-0.492 -0.587	-0.107 -0.074	-0.108 -0.182	-0.467 -0.474	+0.006 -0.026	-0.406 -0.386
$\nabla^2\rho$ (a.u.) [b]	I_{i-1}-I_i	N/A N/A	/ /	+0.029971 /	/ /	+0.020658 /	+0.038407 +0.027065	/ /	+0.029243 /
	I_i-I_{i+1}	+0.025535 /	/ /	/ +0.046341	/ /	/ /	+0.031707 /	/ /	+0.041581 +0.030734
$d(L_{CP}\cdots\rho_{CP})$(Å)	I_{i-1}-I_i	N/A N/A	/ /	0.265 /	/ /	0.018 /	0.695 0.114	/ /	0.248 /
	I_i-I_{i+1}	0.184 /	/ /	/ 0.150	/ /	/ /	0.312 /	/ /	0.714 0.089

I_i		I9	I10	I11	I12	I13	I14	I15	I16	I1	I2
Q (*e*)[a]		-0.183 -0.188	-0.068 -0.072	-0.602 -0.657	-0.058 -0.096	-0.185 -0.122	-0.352 -0.365	+0.009 -0.020	-0.418 -0.426	+0.047 +0.002	-0.237 -0.110
$\nabla^2\rho$ (a.u.) [b]	I_{i-1}-I_i	/ /	/ /	/ +0.038699	/ /	+0.019550 /	+0.042314 +0.037928	/ /	+0.032739 /	/ /	+0.016557 /
	I_i-I_{i+1}	+0.021101 /	/ /	/ +0.032259	/ /	/ /	+0.027737 /	/ /	+0.033982 +0.024432	/ /	N/A N/A
$d(L_{CP}\cdots\rho_{CP})$(Å)	I_{i-1}-I_i	/ /	/ /	/ 0.190	/ /	0.093 /	0.664 0.091	/ /	0.336 /	/ /	0.138 /
	I_i-I_{i+1}	0.091	/	/	/	/	0.235	/	0.623	/	N/A

		/	/	0.171	/	/	/	/	0.170	/	N/A
	[a] : Integrated charges of atoms; first row: isolated chain (vacuum); second row: calculation using PCM (water) [b] : Laplacian value at the $L=-\nabla^2\rho$ interatomic critical points										

Table 16. Topological and geometrical properties at the $L=-\nabla^2\rho$ interatomic critical points of the I1-I2···I3-I4-I5···I6-I7-I8···I9-I10-I11···I12-I13···I14-I15-I16··· I1-I2 chain. First and second lines correspond to values observed at (3,-3) and (3,+1) CP's, respectively.

I_i		I12	I13	I14	I15	I16	I1	I2	I3
Q (*e*)[a]		-0.245 -0.122	+0.049 +0.006	-0.376 -0.360	+0.003 -0.021	-0.390 -0.433	-0.215 -0.160	-0.054 -0.082	-0.562 -0.609
$\nabla^2\rho$ (a.u.)[b]	I_{i-1}-I_i	N/A N/A	/ /	+0.033442 +0.027885	/ /	+0.029089 /	/ /	/ /	/ +0.036784
	I_i-I_{i+1}	+0.016427 /	/ /	+0.032775 /	/ /	+0.042760 +0.033858	+0.021034 /	/ /	+0.041531 +0.041679
$d(L_{CP}\cdots\rho_{CP})$(Å)	I_{i-1}-I_i	N/A N/A	/ /	0.596 0.203	/ /	0.258 /	/ /	/ /	/ 0.195
	I_i-I_{i+1}	0.141 /	/ /	0.298 /	/ /	0.672 0.082	0.113 /	/ /	0.356 0.249

I_i		I4	I5	I6	I7	I8	I9	I10	I11	I12	I13
Q (*e*)[a]		-0.075 -0.075	-0.190 -0.202	-0.451 -0.474	+0.004 -0.026	-0.423 -0.386	-0.099 -0.170	-0.100 -0.071	-0.528 -0.638	-0.007 -0.009	-0.342 -0.168
$\nabla^2\rho$ (a.u.)[b]	I_{i-1}-I_i	/ /	+0.021833 /	+0.041055 +0.029274	/ /	+0.030881 /	/ /	/ /	/ +0.042954	/ /	+0.024073 /
	I_i-I_{i+1}	/ /	/ /	+0.030593 /	/ /	+0.038875 +0.028637	+0.019681 /	/ /	/ +0.026935	/ /	N/A N/A

$d(L_{CP}\cdots\rho_{CP})$(Å)	I_{i-1}-I_i	/ /	0.094 /	0.699 0.092	/ /	0.264 /	/ /	/ /	/ 0.127	/ /	0.173 /
	I_i-I_{i+1}	/ /	/ /	0.292 /	/ /	0.704 0.110	0.015 /	/ /	/ 0.337	/ /	N/A N/A
	[a] : Integrated charges of atoms; first row: isolated chain (vacuum); second row: calculation using PCM (water) [b] : Laplacian value at the $L=-\nabla^2\rho$ interatomic critical points										

Table 17. Topological and geometrical properties at the $L=-\nabla^2\rho$ interatomic critical points of the I12-I13···I14-I15-I16··· I1-I2···I3-I4-I5···I6-I7-I8···I9-I10-I11··· I12-I13 chain. First and second lines correspond to values observed at (3,-3) and (3,+1) CP's, respectively.

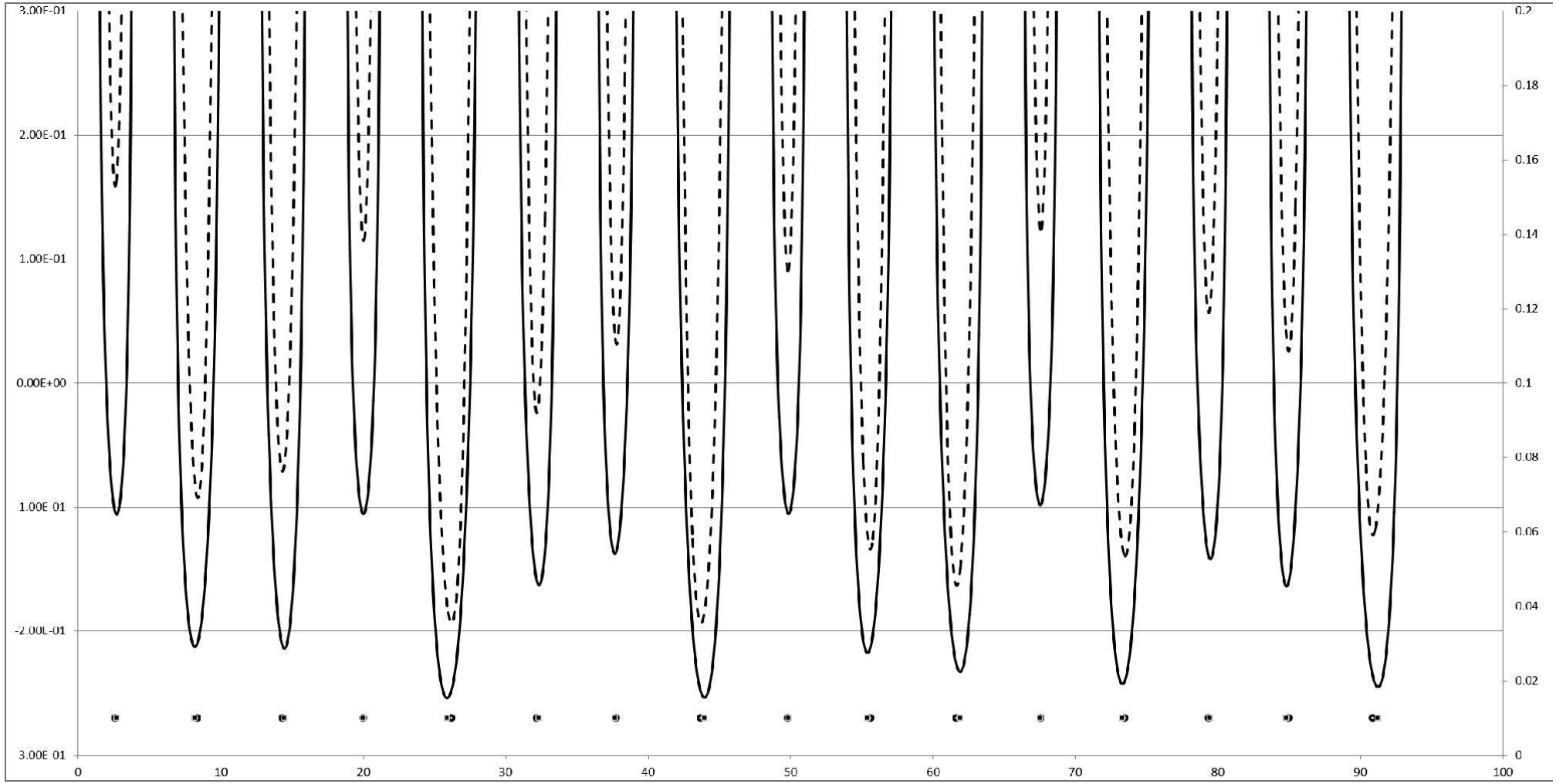

Figure 17: $\phi(\mathbf{r})$ (dashed line) and $\rho(\mathbf{r})$ (solid line) profile along the I1-I2···I3-I4-I5···I6-I7-I8···I9-I10-I11···I12-I13···I14-I15-I16··· I1-I2 chain (a.u. are used).

Positions of minima of $\phi(\mathbf{r})$ and $\rho(\mathbf{r})$ along the chain are marked with open circles and black squares, respectively.

I_i	I1		I2		I3		I4		I5		I6		I7		I8		I9	
Q (*e*)[a]	-0.369		-0.010		-0.492		-0.107		-0.108		-0.467		+0.006		-0.406		-0.183	
d (Å) [b]		-0.096		0.199		-0.147		0.004		0.317		-0.151		0.122		-0.241		
I_i	I9		I10		I11		I12		I13		I14		I15		I16		I1	
Q (*e*)[a]	-0.183		-0.068		-0.602		-0.058		-0.185		-0.352		+0.009		-0.418		+0.047	
d (Å) [b]		-0.039		0.202		-0.244		0.039		0.193		-0.113		0.157		-0.348		

[a]: Integrated charges of atoms

[b]: Distance between closest minima of $\phi(\mathbf{r})$ and $\rho(\mathbf{r})$ along the chain. A positive/negative value means that the $\phi(\mathbf{r})$ minimum is closer to the right/left atom (and then the minimum of $\rho(\mathbf{r})$ is closer to the left/right

Table 18. Integrated charges and distances between $\phi(\mathbf{r})$ and $\rho(\mathbf{r})$ minima along the I1-I2···I3-I4-I5···I6-I7-I8···I9-I10-I11···I12-I13···I14-I15-I16··· I1-I2 chain.

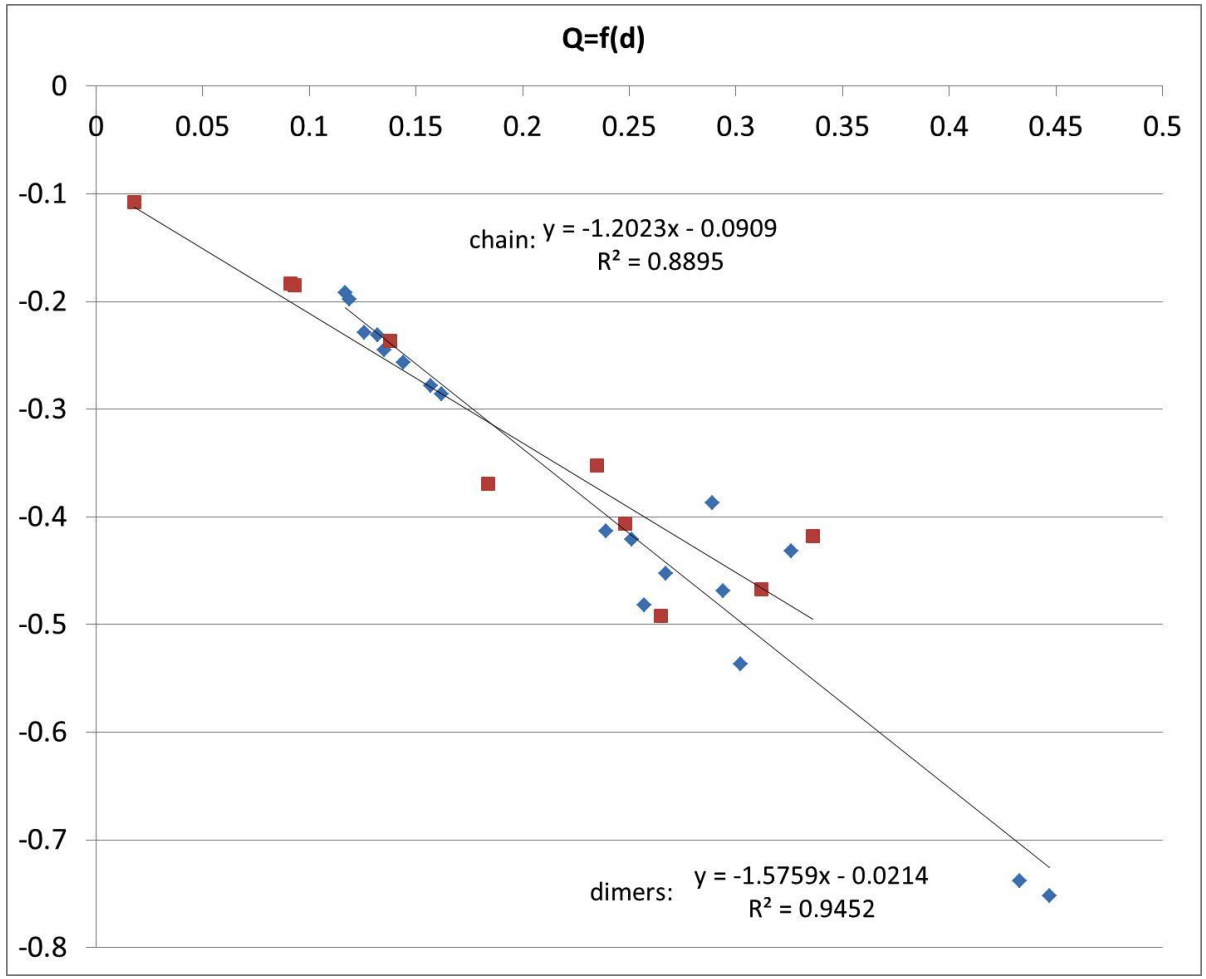

Figure 18. Plot of the atomic integrated charges Q(*e*) as a function of the distance d (Å) between the CP of $\rho(\mathbf{r})$ and $\nabla^2\rho(\mathbf{r})$ observed for I-I interactions in the calculated dimers (blue diamonds) and chain (red squares).

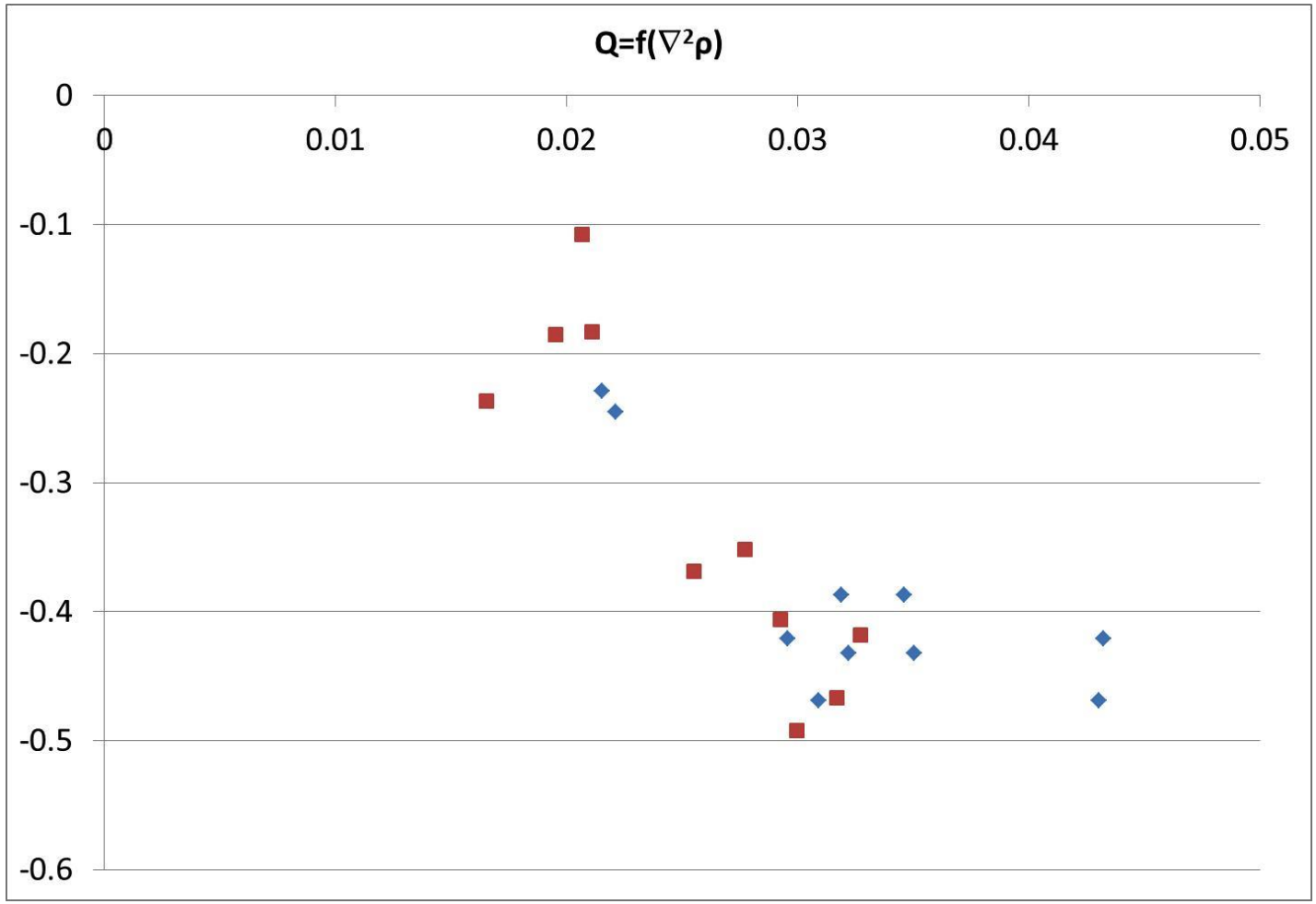

Figure 19. Plot of the atomic integrated charges Q(*e*) as a function of $\nabla^2\rho(\mathbf{r})$ values (a.u.) at $\nabla^2\rho(\mathbf{r})$ CP observed for I-I interactions in the calculated dimers (blue diamonds) and chain (red squares).

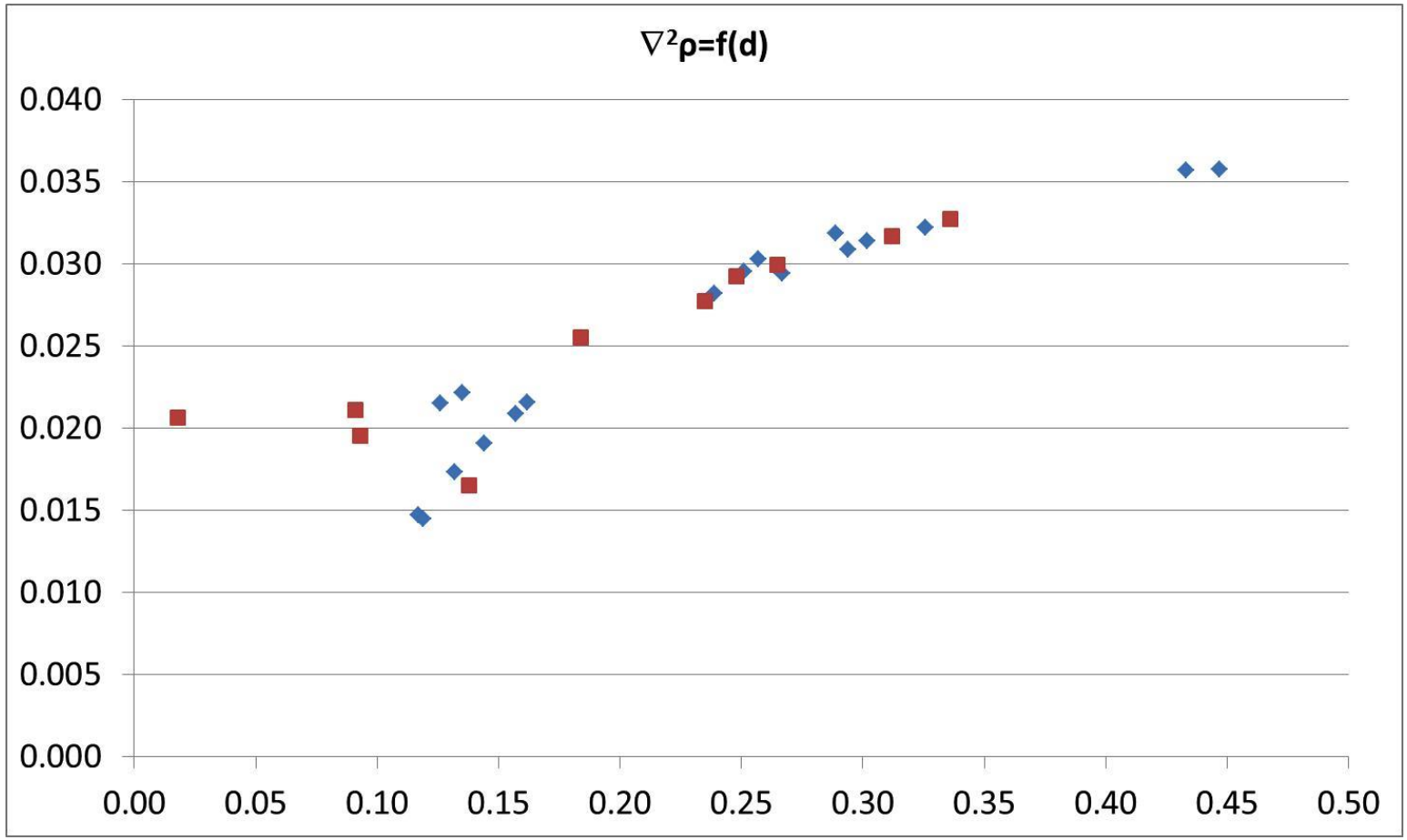

Figure 20. Plot of the $\nabla^2\rho(\mathbf{r})$ values (a.u.) at $\nabla^2\rho(\mathbf{r})$ CP as a function of the distance (Å) between the CP of $\rho(\mathbf{r})$ and $\nabla^2\rho(\mathbf{r})$ observed for I-I interactions in the calculated dimers (blue diamonds) and chain (red squares).

Charges for I_2 molecules	I1-I2 Chains A/B	I4-I5 Chains A/B	I9-I10 Chains A/B	I12-I13 Chains A/B
Vacuum	-0.38/-0.27	-0.22/-0.27	-0.25/-0.20	-0.24/-0.3
with PCM	-0.22/-0.24	-0.26/-0.28	-0.26/-0.24	-0.22/-0.18
Charges for I_3^- anions	I6-I7-I8 Chains A/B	I14-I15-I16 Chains A/B		
Vacuum	-0.87/-0.87	-0.76/-0.76		
with PCM	-0.89/-0.89	-0.81/-0.81		
Charges for I^- anions	I3 Chains A/B	I11 Chains A/B		
Vacuum	-0.49/-0.56	-0.60/-0.53		
with PCM	-0.59/-0.61	-0.66/-0.64		

Table 19. Net atomic charges of the polyiodide chains as calculated from the topology of $\rho(\mathbf{r})$ in the I-basins. Calculations have been carried out in vacuum and with PCM on two alternative chains: A (starting with I1-I2 and ending with I1'-I2') and B (starting with I12-I13 and ending with I12'-I13').

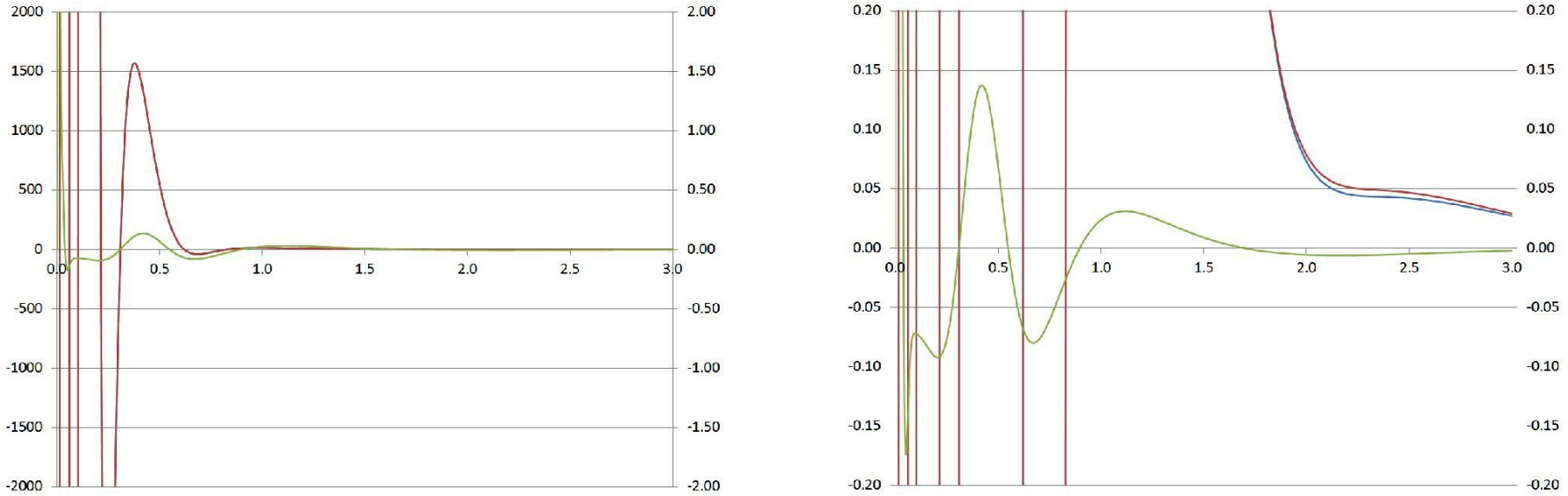

Figure 21. $\nabla^2\rho(\mathbf{r})$ distribution of values (a.u.) along radial directions of isolated I (red) and I^- (blue) species (distance from nucleus in a.u.). The $\nabla^2\rho(\mathbf{r})$ distribution of the difference I^- - I is plotted in green color. Right plot focuses on the very small differences found between I and I^- distributions. In both plots, the vertical scales are: left for I (red) and I^- (blue) species, and right for the difference I^- - I (green). The values of $\nabla^2\rho(\mathbf{r})$ at 2.25 a.u. from I^- and I nuclei (plateau) are 1.07 and 1.21 e.Å^{-5}, respectively. The closest local maximum (VSCD) to the plateau is approximately centered at 0.984 a.u. for both I (378.37 e.Å^{-5}) and I^- (378.88 e.Å^{-5}) species.

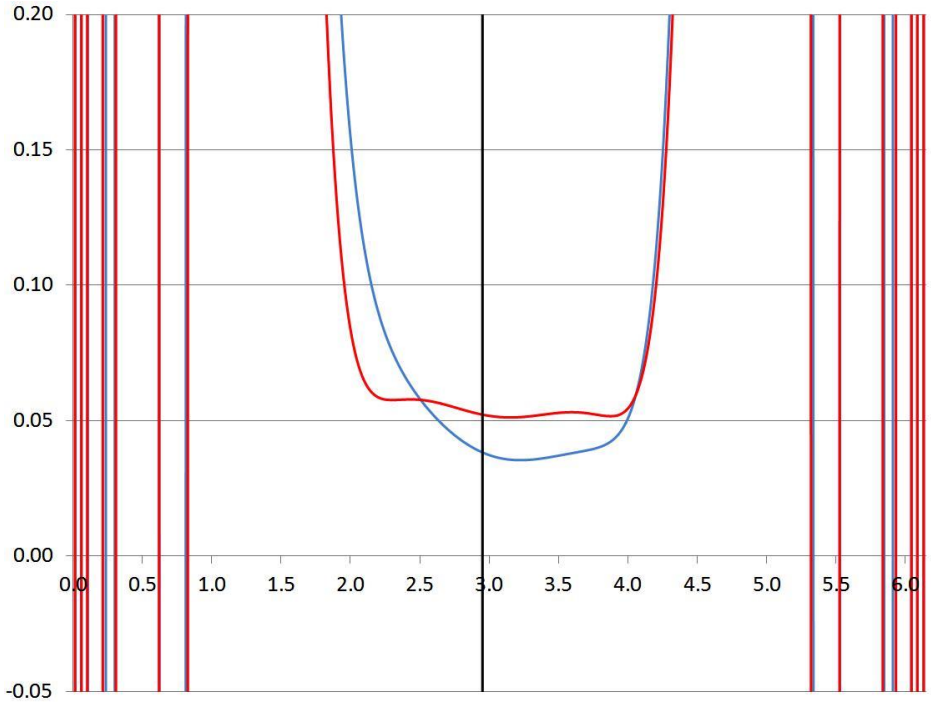

Figure 22. $\nabla^2\rho(\mathbf{r})$ distribution of values (a.u.) along the I2…I3 internuclear direction in the dimer I1-I2…I3-I4-I5 (blue). The extreme positions in the horizontal axis correspond to those of I2 and I3 nuclei (values indicate the distance from the I2 nucleus in a.u.). The position of the bond critical point, and therefore of the interatomic surface, is denoted by the black line. As I2 and I3 are considered iodine and iodide atoms, the $\nabla^2\rho(\mathbf{r})$ distribution observed in their interaction is compared to that of the I…I^- system calculated from the addition of the contributions of isolated I and I- species at the same distance than I2…I3 (superimposed in red). The lower positive $\nabla^2\rho(\mathbf{r})$ magnitude found in the bonding region of I2…I3 indicates a less depleted electron distribution than in I…I- (Independent Atoms Model), resulting from the bonding interaction in the former system.

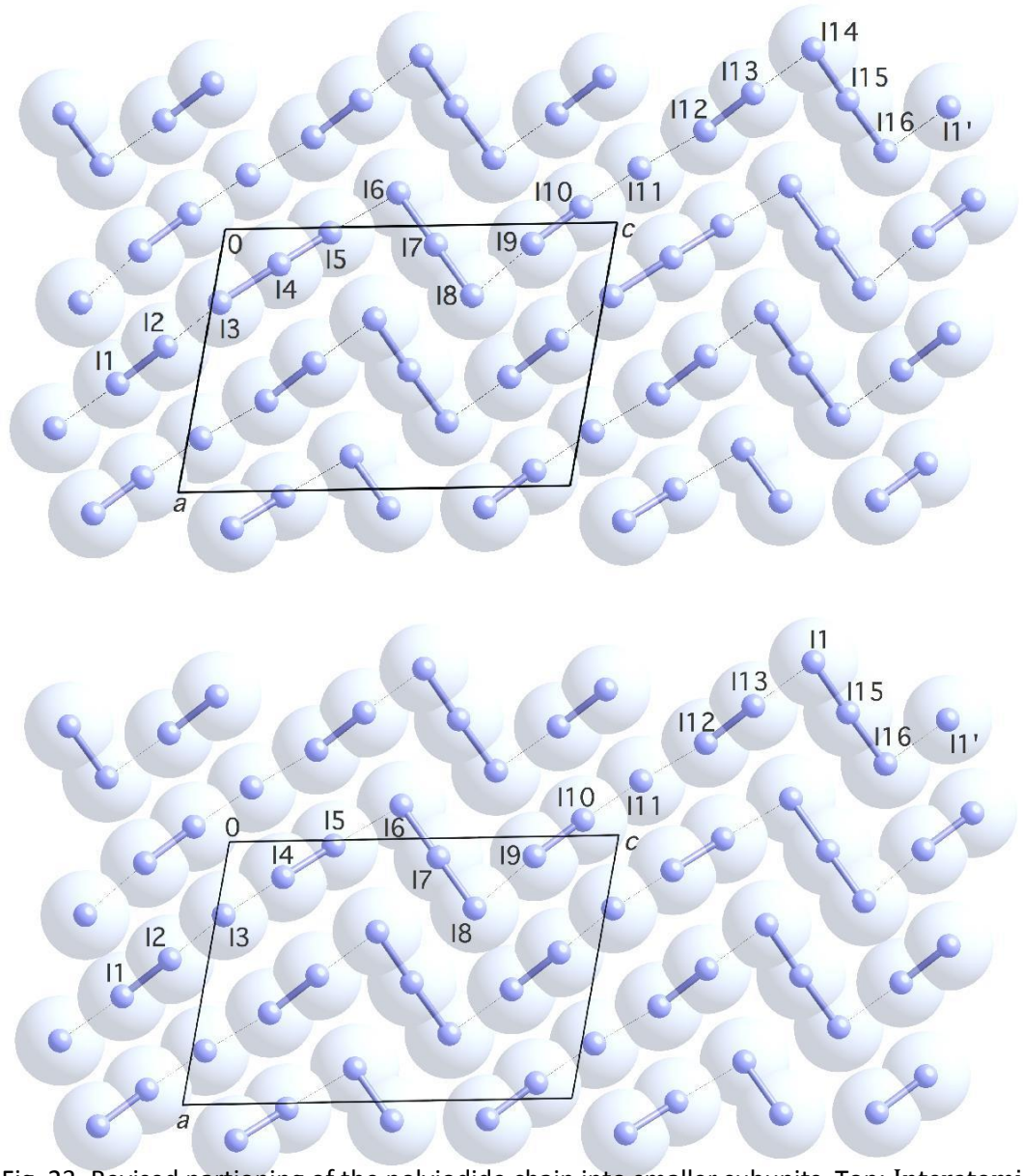

Fig. 23. Revised partioning of the polyiodide chain into smaller subunits. Top: Interatomic distances shorter than 3.2 Å have arbitrarly been drawn as solid lines. Bottom: Cutoff for I-I bonds set to 3.18 Å, in agreement with the results of the topological analysis. Symmetry operator ' = x -1, y, z+2. Note the different assignment of atom I3 according to the two alternative approaches!

References ESI

[1] Gaussian09. Revision D.01, Frisch, M. J.; Trucks, G. W.; Schlegel, H. B.; Scuseria, G. E. , Robb, M.; Cheeseman, J. R.; Scalmani, G.; Barone, V.; Mennucci, B.; Petersson, G. A.; Nakatsuji, H.; Caricato, M.; Li, X.; Hratchian, H. P.; Izmaylov, A. F.; Bloino, J.; Zheng, G.; Sonnenberg, J. L.; Hada, M.; Ehara, M.; Toyota, K.; Fukuda, R.; Hasegawa, J.; Ishida, M.; Nakajima, T.; Honda, Y.; Kitao, O.; Nakai, H.; Vreven, T.; Montgomery, Jr. J. A.; Peralta, J. E.; Ogliaro, F.; Bearpark, M.; Heyd, J. J.; Brothers, E.; Kudin, K. N.; Staroverov, V. N.; Keith, T.; Kobayashi, R.; Normand, J.; Raghavachari, K.; Rendell, A.; Burant, J. C.; Iyengar, S. S.; Tomasi, J.; Cossi, M.; Rega, N.; Millam, J. M.; Klene, M.; Knox, J. E.; Cross, J. B.; Bakken, V.; Adamo, C.; Jaramillo, J.; Gomperts, R.; Stratmann, R. E.; Yazyev, O.; Austin, A. J.; Cammi, R.; Pomelli, C.; Ochterski, J. W.; Martin, R. L.; Morokuma, K.; Zakrzewski, V. G.; Voth, G. A.; Salvador, P.; Dannenberg, J. J.; Dapprich, S.; Daniels, A. D.; Farkas, O.; Foresman, J. B.; Ortiz, J. V.; Cioslowski, J. and Fox, D. J.: Gaussian, Inc., Wallingford CT, 2010

[2] K. A. Peterson, B. C. Shepler, D. Figgen, H. Stoll, Journal of Physical Chemistry A 110, 13877 (2006).

[3] AIMAll, Todd A. Keith, TK Gristmill Software, Overland Park KS, USA, 2014 (aim.tkgristmill.com).